Construction and Building Materials 242 (2020) 118121

Contents lists available at ScienceDirect

Construction and Building Materials

journal homepage: www.elsevier.com/locate/conbuildmat

Experimental study on effect of resin matrix in basalt fiber reinforced polymer composites under static and fatigue loading

Xing Zhao [a], Xin Wang [b,c,*], Zhishen Wu [b,c,*], Jin Wu [a]

[a] Department of Civil Engineering and Airport Engineering, Nanjing University of Aeronautics and Astronautics, Nanjing 211106, China
[b] Key Laboratory of C & PC Structures Ministry of Education, Southeast University, Nanjing 210096, China
[c] National and Local Unified Engineering Research Center for Basalt Fiber Production and Application Technology, International Institute for Urban Systems Engineering, Southeast University, Nanjing 210096, China

HIGHLIGHTS

- Matrix played important roles in both of the static and fatigue for BFRP.
- Same static but lower fatigue strength for vinyl ester based than epoxy based BFRP.
- Static strength was lower with more ductile matrix based BFRP.
- Long-term fatigue life increase with increase in fracture elongation of the resins.

ARTICLE INFO

Article history:
Received 25 October 2019
Received in revised form 26 December 2019
Accepted 6 January 2020

Keywords:
Resins
Static behavior
Fatigue performances
Fatigue damage
Basalt fiber reinforced polymer composites (BFRP)

ABSTRACT

To reveal the effect of resin matrix on the behavior and damage mechanism of basalt fiber reinforced polymers (BFRPs), the static and fatigue properties of different resin matrixes based BFRP composites were experimentally investigated. Four types of resins were adopted in this paper. They were normal and toughened vinyl ester resins, and epoxy systems curing at room temperature and at elevated temperature. In parallel to the static and fatigue tests, the damage observation were conducted using in-situ scanning electron microscopy (SEM) observation system embedded in the fatigue test equipment. The results showed that the resins played important roles in both of the static and fatigue behavior of BFRP composites. The static tensile strength of the normal vinyl ester resin based BFRP was similar to that of the BFRP with elevated temperature cured epoxy. However, the fatigue life of the former was significantly lower than that of the latter for more matrix cracking and fiber peeling occurred on the surface of the vinyl ester resin based BFRP. Although the static strength of the BFRP was lower with more ductile matrix like toughened vinyl ester or room temperature cured epoxy, the long-term fatigue strength level of BFRP increased with an increase in fracture elongation of the resins.

1. Introduction

During the last few decades, basalt fiber reinforced polymer (BFRP) has gotten increasing attentions in both industrial and academic world for its superior mechanical properties compared to glass fiber reinforced polymer (GFRP) and less costs than carbon fiber reinforced polymer (CFRP) [1–5]. The creep and fatigue properties of BFRPs is higher than that of GFRP composites [6,7]. BFRPs are promising materials for structures which are sensitive to fatigue loading [8,9].

Although the mechanical properties of fiber reinforced polymer (FRP) materials are mainly determined by fiber properties, the fatigue properties of the composite materials varied for different matrices [10–13]. Several studies have investigated the effect of the resin on mechanical especially fatigue properties of FRP laminates. Rassmann et al.[14] used different resin systems and compared the mechanical and water absorption properties of kenaf fiber and glass fiber reinforced polyester, vinyl ester and epoxy laminates. The results showed that the various resins had differing effects on FRP strength and hence different failure modes. Colombo et al. [15] studied the static and fatigue properties of BFRP laminates with vinylester and epoxy matrices and found that the mechanical properties of basalt reinforced epoxy composites were superior to those of vinyl ester and the macroscale failure modes were more compact. The results of other studies investigating

* Corresponding authors at: Key Laboratory of C & PC Structures Ministry of Education, Southeast University, Nanjing 210096, China.
E-mail addresses: xinwang@seu.edu.cn (X. Wang), zswu@seu.edu.cn (Z. Wu).

https://doi.org/10.1016/j.conbuildmat.2020.118121
0950-0618/

different resin toughening methods have also shown that the properties of the matrix have certain impacts on the fatigue behavior of FRPs, and that fatigue behavior is improved by using toughened resins [16–19]. However, the resins used for FRP laminates are usually not suitable for pultruded products like BFRP tendons, cables or profiles. Limited studies can be found on the effect of resins on static/fatigue behavior and damage of pultruded products.

With the aim of optimizing resins used in BFRP materials that are employed in pultruded fatigue sensitive structural members, this study focuses on evaluating the effect of resins on the static/fatigue behavior and damage mechanism of BFRP composites. The strength, fatigue life, and micro damage mechanism of four different types of resin-based BFRP composites were clarified using advanced fatigue testing equipment combined with an in-situ scanning electron microscope (SEM). Except for the epoxy system curing at room temperature, the other resins studied in this work, the epoxy curing at elevated temperature, the normal vinyl ester and the toughened vinyl ester, were all suitable for pultruded products like BFRP tendons, cables or profiles. Use of the in-situ SEM enabled both the fracture surface and the evolution of micro damage to be studied.

2. Materials and experimental setup

2.1. Materials and specimens preparation

In this study, systems of continuous longitudinal basalt fibers reinforced composite were investigated based on basalt fibers treated with silane sizing obtained from Jiangsu Green Materials Valley New Material T&D Co., Ltd (GMV). The tensile strength, elastic modulus and fracture elongation of the basalt fiber provided by the manufacturer were 2400 MPa, 90 GPa and 2.2%, respectively. Four types of resin were applied. They were normal vinyl ester Corrolite 9102-70 from Reichhold Polymers (Tianjin) LTD., toughened vinyl ester MFE-9 from Sino Polymer Co., epoxy 9804A/B from Bluestar Wuxi Petrochemical Co. and epoxy L-500AS/BS from Sanyu Rec Co., Ltd., respectively. Except for epoxy L-500AS/BS, they are resins used in pultrusion process, which are usually cured at elevated temperature. The epoxy L-500AS/BS, epoxy system curing at room temperature, was applied here to investigate the effect of epoxy systems of different curing temperature.

The mean values of mechanical properties of resins obtained from tensile tests of resin casting body by the authors' group are listed in Table 1. It can be seen that the elastic modulus of the epoxy resins is slightly higher than that of the vinyl resins and the largest difference between their mechanical properties relates to fracture elongation. A large increase in the strength and elongation of the toughened vinyl ester can be found compared with the normal vinyl ester. The fracture elongation of the toughened vinyl ester is even higher than that of the epoxy resins. It also should be noted that the toughened vinyl ester is toughened using elastic nanoparticles which can prevent small resin cracks from extending but cannot prevent small cracks from forming. When compared with epoxy systems cured at elevated temperatures, the epoxy system cured at room temperature exhibits greater fracture elongation which can relate to the larger plasticity of the resin.

2.2. Specimen preparation and test setup

The shape and size of the specimens used in the tests were identical to those used in the authors' previous studies [13,21]. Each specimen consisted of two parts: a pre-impregnated continuous basalt fiber bundle and end tabs (to smooth the stiffness change and minimize the risk of tab failure during fatigue testing). The pre-impregnated basalt fibers bundle of 1200 tax was first wound onto a flat mold to form a continuous and straight tow-preg bundle with a width of approximately 3 mm and a thickness of approximately 0.25 mm. Four end tabs were then adhered to the bundle, leaving a gauge length of 20 mm. Each tab consisted of one outside layer of basalt fiber sheet, and one inside layer sheet stretched out to a distance of approximately 10 mm from the outside layer. After post-curing (curing conditions are listed in Table 2), the specimens were cooled in air and then cut into a dumbbell shape with a total length of 70 mm. Prior to testing, the specimens were cleaned with absolute ethanol and coated with a thin platinum layer in a JEOL JFC-1600 sputter coater to assist with SEM observations.

Both quasi-static and the fatigue tests were conducted using a Shimadzu SEM Servopulser, which combines a hydraulic servo fatigue drive and an in-situ SEM device. This loading, observing and gripping devises used in this study were identical to that in authors' previous studies [13,21], which was proved to be suitable for testing BFRP composites. For the quasi-static tests, 5 replicas were tested for each set at a stroke rate of 2 mm/min. The stress of all specimens was calculated by machine load / cross-sectional area of fiber yarn in the FRP according to ISO standard [22]. Fatigue tests were conducted under a constant stress amplitude cyclic load at room temperature (some control parameters used in the fatigue testing are listed in Table 2). The specimens were tested until failure occurred at N_f cycles or until run-out cycles (1×10^7 cycles). 3 replicas were adopted for each fatigue test. The stiffness of the specimens was defined as (maximum load – minimum load)/(maximum deformation – minimum deformation), and the values were recorded for each cycle during fatigue loading.

Table 1
The properties of the resins.

Resins	Tensile strength (MPa)	Elastic modulus (GPa)	Fracture elongation (%)
Normal vinyl ester (Corrlite 9102-70)	44.81	3.13	1.58
Toughened vinyl ester (MFE-9)	67.38	2.93	5.38
Epoxy System Curing at Elevated Temperature (9804A/B)	76.29	3.44	2.87
Epoxy System Curing at Room Temperature (Sanyu L-500AS/BS) [20]	52.9	2.90	3.63

3. Experimental results and discussion

3.1. Static tensile properties

The results of static tests are shown in Table 3, where the static strengths of BFRP with different resin matrixes are seen to be all above 2300 MPa. These values are all higher than the strength of E-glass FRP sheets (1600–2300 MPa) but lower than the strength of carbon FRP sheets (3830–6600 MPa) [25–27]. The toughened vinyl matrix based composites had the lowest strength which was 84% of the highest strength achieved in normal vinyl ester based BFRPs. The static strength of BFRP cured at room temperature (BSE) was 91% of that of the 9804A/B epoxy based BFRP (BE). The strength of the BFRP decreased with an increase in the fracture elongation of the matrix. This strength decrease phenomenon of more ductile matrix has also been found in other studies involving matrix toughening, and it is possibly attributed to lowering of the crosslinking density of the toughening systems [16,17].

BFRP products with epoxy resin usually have better mechanical properties than those with vinyl ester [15,28]; however, the static strengths of the BE specimens were slightly lower than those of BV specimens in this test. The BV specimens in this study were small enough to allow the fibers evenly take an even load with a good anchorage, and this mechanism would be discussed later in the paper with respect to fracture observations.

The stress-displacement curves of different resin matrixes specimens are shown in Fig. 1. The stress–strain curves of BFRP (besides BV) were linear with a sudden drop after failure, which is typical of a FRP stress–strain curve [29]. When the BV specimens approached the maximum load, there was an obvious increase in the displacement without a significant load drop. This indicates that the failure of the vinyl specimen was caused by uneven fiber fracture and peeling, which would be further discussed later in the paper with respect to fracture observations.

The macroscale fracture of specimens had a broom-like appearance with fibers blasted out (as shown in Fig. 2), which is the desirable fracture mode for static tests. The degree of the blast-out varied between the different resin-based BFRPs. The BV specimen was completely blasted out into single fibers, whereas the BRV specimen after failure was relatively integrated, and some bundles of fibers were still evident; however, the BE and BSE specimens were even more integrated than the fractured BRV specimen.

The typical microscale failure patterns of different resins based BFRPs are shown in Fig. 3. Fig. 3(a) shows that the fibers were completely blasted out and no integrated fiber bundles remained with

Table 2
Test programs.

Specimen	Matrix	Curing conditions	Stress ratios	Frequency	Run-out
BV	Normal vinyl ester	2 h 200 °C	0.8*1	10 Hz*2	1×10^7
BRV	Toughened vinyl ester	2 h 200 °C			
BE	Epoxy System Curing at Elevated Temperature	2 h 200 °C			
BSE	Epoxy System Curing at Room Temperature	7d 25 °C			

*__Note__: 1. The ratio of maximum and minimum tension forces in the cables of cable-stayed bridge under traffic load and dead load is about 0.8 [23].
2. The fatigue properties will not be affected if the load frequency is less than 10 Hz, and thermal effect of the fatigue load at 10 Hz can be neglected [24].

Table 3
Ultimate tensile strength (UTS) of different resins based BFRP.

	BV	BRV	BE	BSE
Mean value of UTS (MPa)	2652	2233	2613	2383
COV (%)	4.92	3.60	3.08	2.86

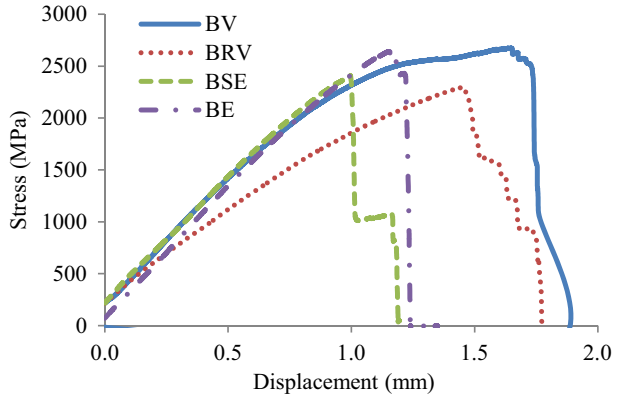

Fig. 1. Stress-displacement curves of different BFRPs.

failure of the BV specimen. The matrix of the vinyl ester cracked into pieces, and each fiber peeled off into loose fibers. Each fiber remained anchored to the end tabs as the specimen was small and with good anchorage, therefore, the fibers could be held together at the end. The specimen could carry a load with fiber peeling until catastrophic fiber breaking. For toughened vinyl ester based BFRP, some fibers were blasted out and intact matrices were still visible, as shown in Fig. 3(b), which was the result of reduced matrix cracking. For epoxy based BFRPs (Fig. 3(c)–(d)), bundles of fibers were pulled out, and fractured fibers can be seen wrapped up in the matrix.

3.2. S-N curves

Fatigue experiments were conducted on the BFRP composites at different maximum stresses and the fatigue results are shown in Fig. 4. The results are clearly scattered, which is expected for FRP composites [26,27]. Composite materials are known to have varying fatigue life lengths, as there are statistical variations in the damage rate that develops [26]. It can be seen that the fatigue life of BE was higher than that of BV, although the tensile strengths of BE and BV were similar. Fig. 4 also shows the linear fitting S–log(N) relationships calculated from the test data using the least-square method according to Eq. (1) [30],

$$\sigma_{\max} = A\log(N_f) + B \tag{1}$$

where $\sigma_{\max}$ represents the maximum fatigue stresses, N_f represents the corresponding number of cycles to failure, and A and B are model parameters that will be determined by the available fatigue data. Data relating to specimens that did not show failure in the fatigue tests are not included in the curve fitting. The fitting results were shown in Fig. 4 and Table 4. The coefficients of determination of the fitting are less than 0.9 because of damage pattern shift for low-cycle fatigues and high-cycle fatigues, which have been discussed in the authors' previous studies [13].

The slope of the S–N fatigue curve, which can be indicated by parameter A, was steepest for BV specimens. This characterizes that BV specimens had the fastest degradation in fatigue strength with fatigue life. Toughed vinyl ester resin based BFRP (BRV) has the lowest absolute value of parameter A, which indicates that the fatigue properties of toughed vinyl ester resin based BFRP were improved. The slopes of the S–N fatigue curves for epoxy based BFRPs were between those of BV and BRV, where BSE obtained a lower value than BE.

The static tensile strengths for different resins based BFRPs were varied. Normalized with the tensile strengths, Fig. 5 presents the linear fitting stress levels–log(N) relationships calculated from test data using the least-square method according to Eq. (2) [30].

$$r_{\max} = \frac{\sigma_{\max}}{\sigma_{ult}} = A_r\log(N_f) + B_r \tag{2}$$

where $r_{\max}$ represents the stress level (ratio of maximum fatigue stresses, $\sigma_{\max}$, to ultimate strength, σ_{ult}), N_f represents the corresponding number of cycles to failure and A_r and B_r are the model parameters determined by the available fatigue data.

The fitting results were shown in Fig. 5 and Table 5. At the same stress levels, the life of the toughened BRV specimen was much longer than that of BV specimens, and the difference in life lengths between BRV and BV increased with a decrease in stress levels. This result indicates that optimizing resin toughness can improve fatigue resistance of BFRP. The fatigue degradation mechanism is discussed later in the paper with respect to damage observations.

The fatigue strength and life of different resin type based BFRP materials can be predicted using the S-N curves. The prediction results are presented in Table 6. For BE, the predicted fatigue strength to achieve a 10 million cycle life is 2025 MPa, and the fatigue strength level is 77.51%. These results are much higher than those of BV (1954 MPa and 69.89%). Toughened vinyl ester based BFRP has a lower fatigue strength than vinyl matrix based BFRP for fatigue life of 2 and 10 million, which is due to the lower static strength of toughened vinyl based BFRP. However, the fatigue strength level for 10 million cycles increased from 69.89% to 75.56% for normal and toughened vinyl ester based BFRPs because static strength had been used to normalize the fatigue performance. For longer cycles, such as 10^{13} cycles, the fatigue strength levels predicted for BRV materials were highest because the slope of its S-N curve was lowest.

3.3. Stiffness degradation

The stiffness reduction can be an indicator of damage during fatigue loading, which usually be divided into three region, (I) multiple crack initiation during the first 20% of fatigue life, (II) slow and

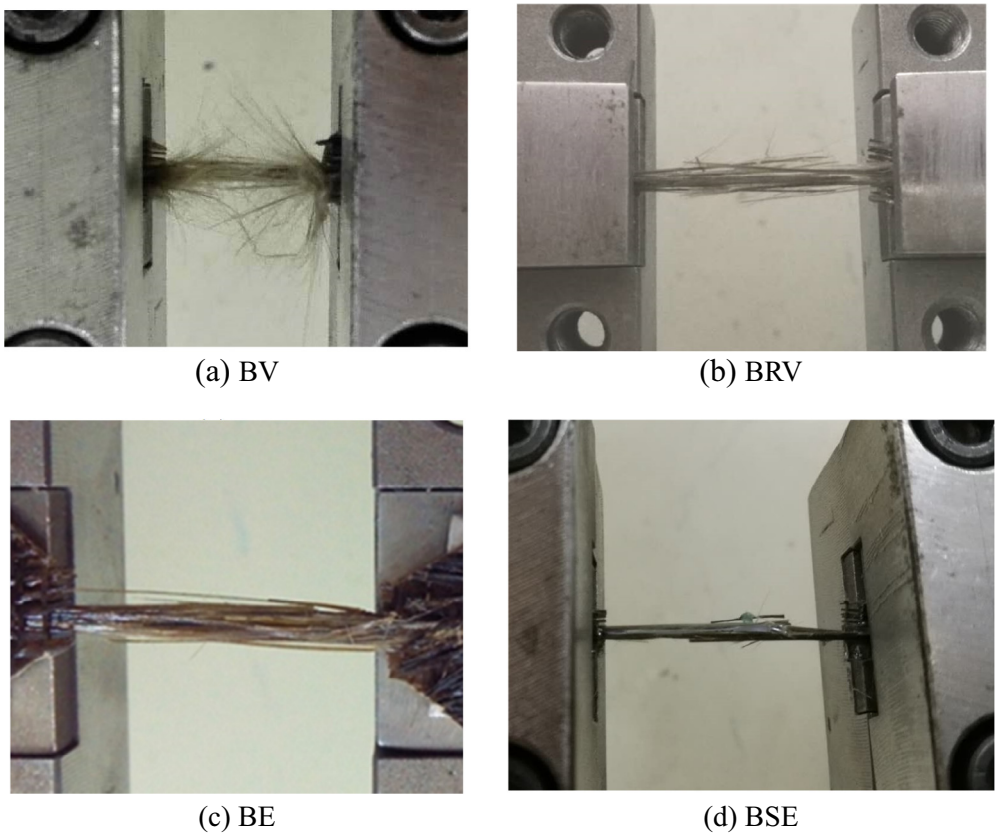

(a) BV (b) BRV

(c) BE (d) BSE

Fig. 2. Typical macroscale failure patterns of different resins based BFRPs.

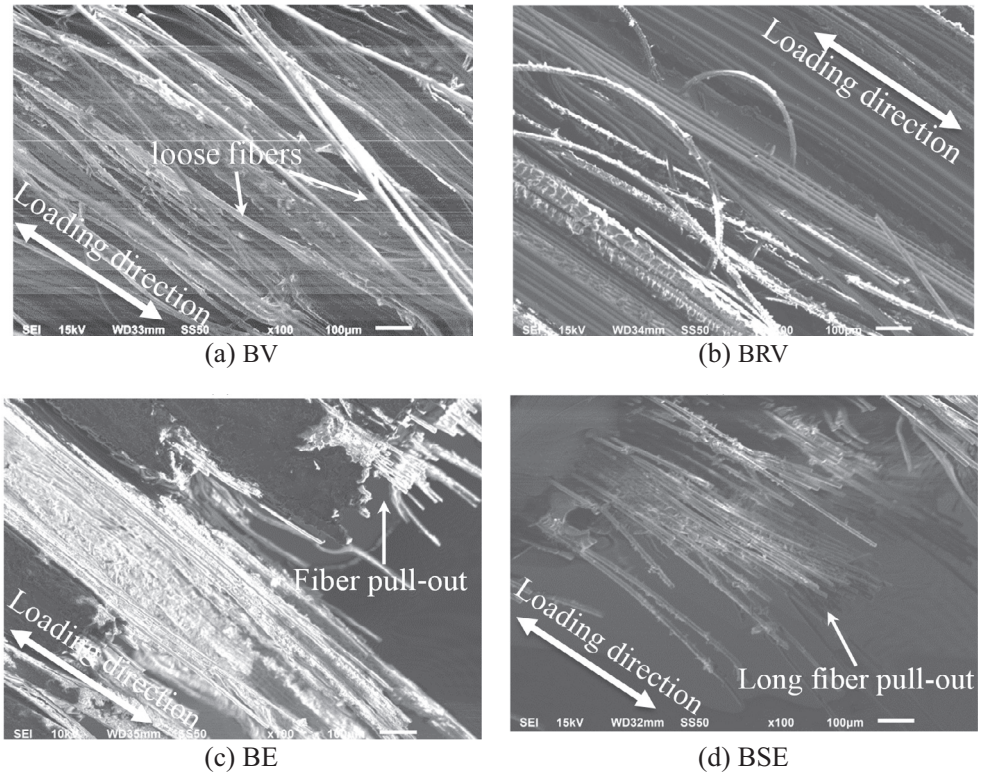

(a) BV (b) BRV

(c) BE (d) BSE

Fig. 3. The typical failure surface of static test.

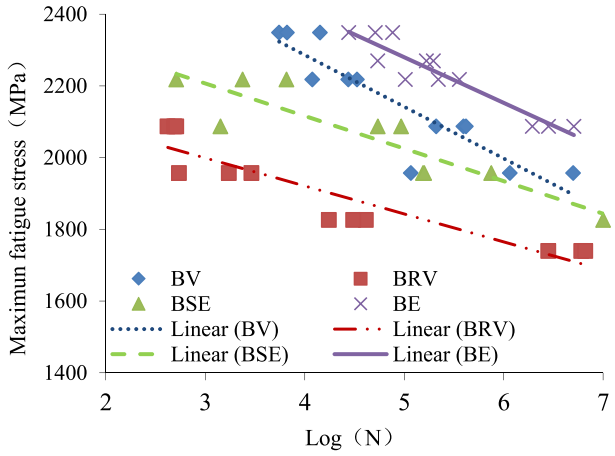

Fig. 4. Maximum fatigue load S- life N curves.

Table 4
Fitting parameters of maximum fatigue load S- life N curves of different resins based BFRPs.

Specimen	Parameters		Coefficients of determination R^2
	A	*B*	
BV	−144.15	2862.5	0.80
BRV	−77.807	2231.9	0.81
BSE	−90.805	2478.8	0.85
BE	−127.14	2915.4	0.88

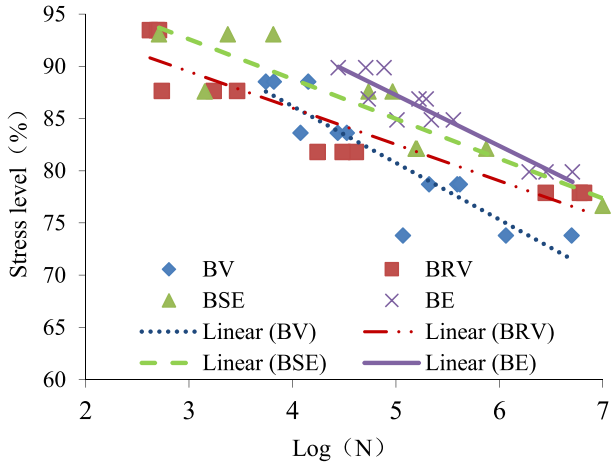

Fig. 5. Maximum stress levels–life N curves.

Table 5
The fitting parameters of maximum stress levels–life curves different resins based BFRPs.

Specimen	Parameters		Coefficients of determination R^2
	A_r	B_r	
BV	−5.4357	1.0794	0.80
BRV	−3.4844	0.9995	0.81
BSE	−3.8105	1.0402	0.85
BE	−4.8655	1.1157	0.88

stable crack grow along the fiber–matrix interface and (III) fiber breaking within a short life span immediately prior to failure [11,13,27,31,32]. Fig. 6 shows typical normalized stiffness degradation of different resins based BFRP composites with respect to the normalized fatigue cycles, and the results basically following the three region model.

Stiffness degradation at 20%, 50% and 90% of the fatigue life of different resins based BFRPs during fatigue were compared to study the behavior of different resins based BFRP materials during fatigue in the three regions, as shown in Fig. 7. At 20% of fatigue life, there was evidently less stiffness degradation for the toughened BRV specimen under the same maximum fatigue stress (compared to the non-toughened BV specimen) in region I. This shows that the toughened BRV exhibited comparatively less crack damage. However, the difference between these specimens in region I was small because the fiber (rather than the matrix) mainly contributes to stiffness in unidirectional BFRP. At 90% of fatigue life, a larger difference was observed in region III; greater degradation was observed in BRV and BSE than in BV and BE. This shows that BFRP with matrices that were more ductile were more damage tolerant than the more brittle resin-based BFRPs. The damage mechanism is discussed in the next section.

3.4. SEM observation

3.4.1. Normal vinyl ester based BFRP (BV)

Fiber peeling was clearly seen during the fatigue process of the vinyl BFRP specimen, as shown in Fig. 8(a), and it was also completely blasted during fatigue failure, as shown in Fig. 8(b).

From a microscopic damage perspective, the fiber peeling of the vinyl BFRP specimen was related to a large amount of cracks in the vinyl resin on the surface of fibers (as shown in Fig. 9(a)). With an increase in the number of cycles, the numbers and lengths of resin cracks increased (as shown in Fig. 9(b)–(c)), and the resin was ultimately disconnected from the fibers (as shown in Fig. 9(d)).

3.4.2. Toughened vinyl ester based BFRP (BRV)

Typical fatigue damage of toughened vinyl BFRP specimens shows that the ductility of toughened vinyl resin was greater than that of vinyl ester resin. There was an evident decrease in the number of cracks with the same cycle times at the same load as shown in Fig. 9(a) and Fig. 10(a). When toughened vinyl BFRP finally failed, a large number of resin particles remained on the fiber bundles, which did not occur with the vinyl BFRP, and this indicates that the fibers had not completely peeled off in the toughened vinyl ester based BFRPs. In addition, when toughened vinyl ester based BFRP was fractured, the specimen (Fig. 10(d)) did not blast out into separate fibers (unlike the BV specimens) (Fig. 9(d)).

3.4.3. Epoxy system curing at elevated temperature based BFRP (BE) and at room temperature based BFRP (BSE)

As the viscosity of the epoxy at room temperature is higher than that at elevated temperature, the basalt fibers were wrapped up with a greater amount of resin in the BSE specimens than in BE specimens. The SEM images of BSE specimens in Fig. 11(a) show a smooth surface with some cutting fragments thereon, and it is difficult to observe any fibers. From the counterpart of BE specimens in Fig. 11(b), many fibers can be seen embedded in the resins on the surface. The damage pattern were the same matrix cracking damage for both BSE and BE, but the size of cracks in BSE is a little smaller than that in BE as shown in Fig. 11(c)–(d). That is the reason of slower fatigue life degradation of BSE than that of BE.

It is also of note that less matrix cracking occurred in BSE than in BRV, but fracture elongation was lower in the former than the latter. This is because the toughened vinyl ester is toughened by elastic nanoparticles that prevent any small resin cracks from extending, but they cannot prevent small cracks from forming.

Table 6
The fatigue strength prediction of different resins based BFRPs.

	Fatigue strength (MPa)			Fatigue strength level (%)		
	2×10^6 cycles life	1×10^7 cycles life	1×10^{13} cycles life	2×10^6 cycles life	1×10^7 cycles life	1×10^{13} cycles life
BV	1954	1853	989	73.70	69.89	37.28
BRV	1742	1687	1220	78.00	75.56	54.65
BSE	1907	1843	1298	80.01	77.35	54.48
BE	2114	2025	1263	80.92	77.51	48.32

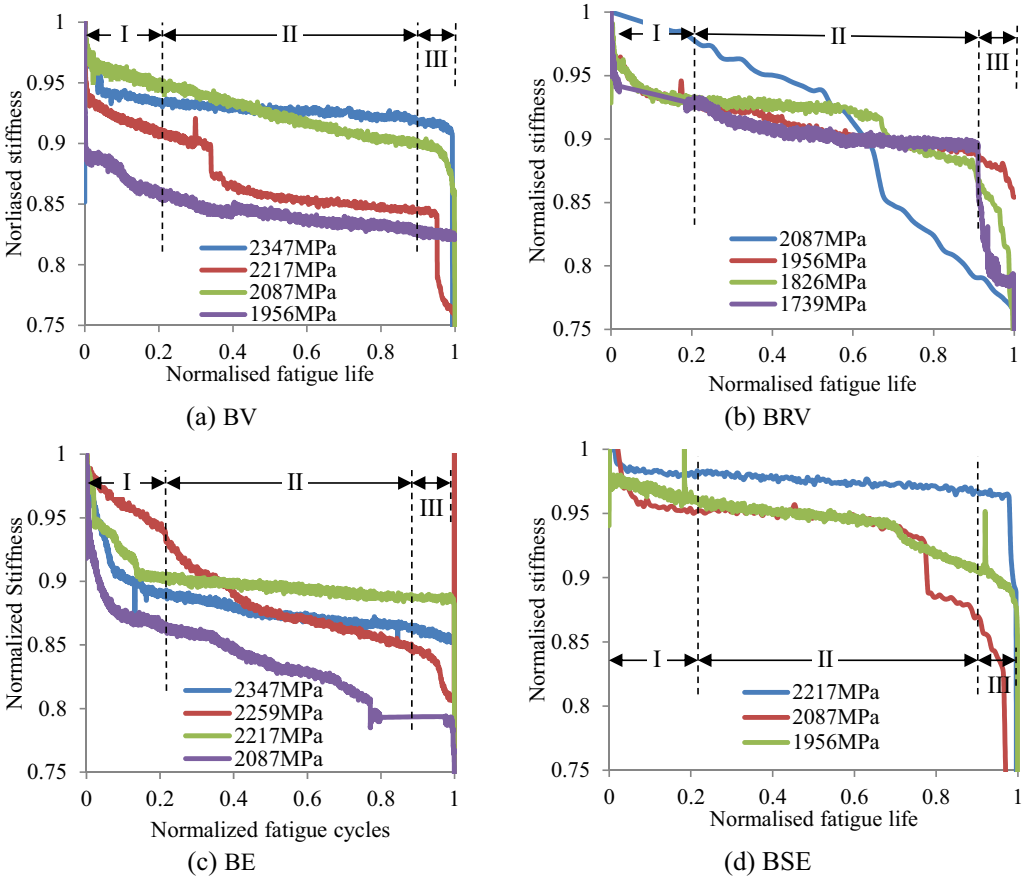

Fig. 6. Typical normalized stiffness degradation curves for different resins based BFRP.

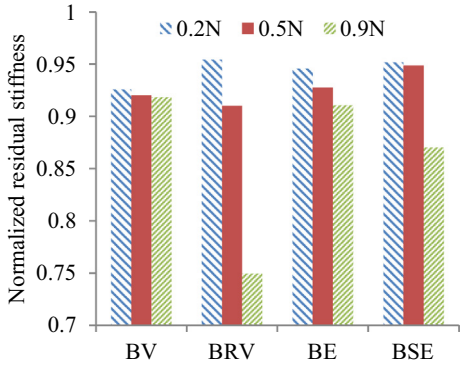

Fig. 7. Typical normalized residual stiffness for different resins based BFRP at 20%, 50% and 90% of fatigue life (0.2 N, 0.5 N and 0.9 N) under maximum fatigue stress of 2087 MPa.

3.5. Fatigue damage mechanism analysis

Compared with the epoxy matrices based BFRP, the normal vinyl ester matrix was easier to crack and fiber was easier to be peeled off in BV during fatigue loading, as shown in Fig. 9 and Fig. 11. The peeled off fibers in BV specimens gradually withdrew from working during fatigue cycles. This results in more fibers being peeled off with an increased cyclic load. When actual stress of the residual fibers increased to its fracture limit, the BV specimens failed. With less matrix cracking and fiber peeling, the epoxy matrices based BFRPs had much higher fatigue life.

Polymer matrix ductility and cracking can affect the fatigue failure mechanisms of FRP composites, and the long-term fatigue limit of unidirectional composite is around fatigue limit of matrix [10–12]. As shown in Fig. 12, the slope of the S–N fatigue curve increases with polymer matrix elongation. The SEM images (Figs. 9–11) show more ductile matrixes based BFRPs like BRV

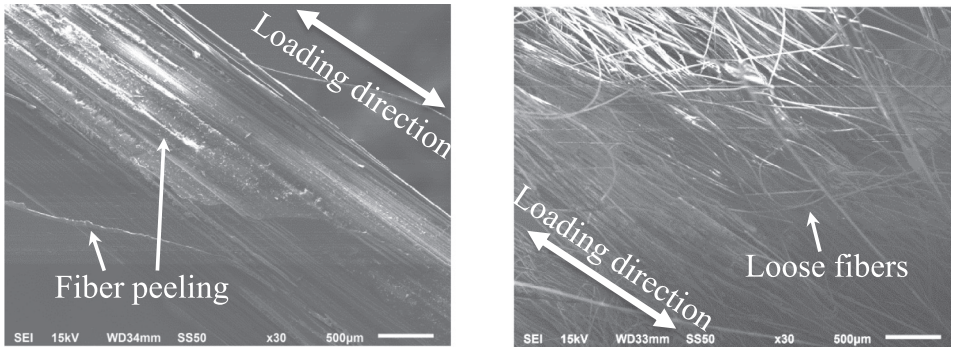

（a）100000 cycles （b）393907 cycles

Fig. 8. Typical damage (×30) for BV under maximum fatigue stress of 2087 MPa.

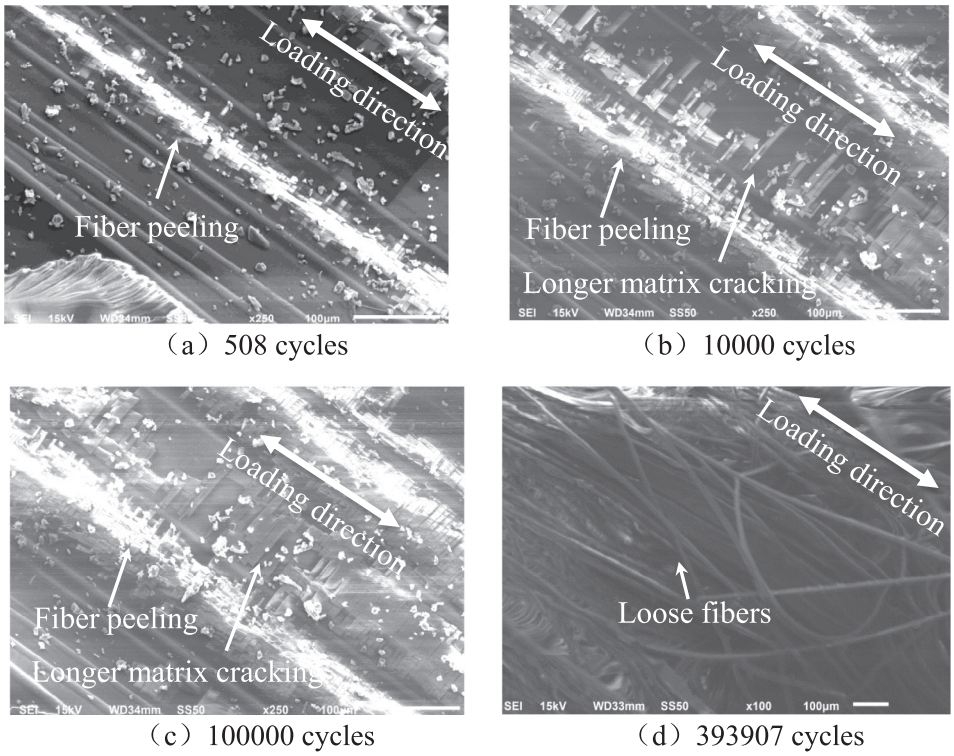

（a）508 cycles （b）10000 cycles

（c）100000 cycles （d）393907 cycles

Fig. 9. Typical damage for BV under maximum fatigue stress of 2087 MPa.

and BSE have smaller or less cracks damage than BV and BE. This smaller and less fatigue damage can result in a reduced degradation rate of both fatigue life and initial stiffness.

4. Conclusions

In this study, the effects of resin matrix on the static properties, fatigue behavior, and damage mode of BFRP were investigated with static and fatigue tests combined with in-situ SEM observation. Four different types of resin-based BFRP composites were applied in the test. They are normal and toughened vinyl ester resins, and epoxy systems curing at room temperature and at elevated temperature. The primary findings of this paper are summarized as follows:

1) The vinyl resin-based BFRP has a similar static strength to the epoxy curing at elevated temperature based BFRP, but the former has a much lower fatigue life than the latter. The failure modes of fiber peeling and fiber pull-out are found for the vinyl resin-based and the epoxy based specimens, respectively. The peeled off fibers can sustain the static load with good end anchorage, while the peeled off fibers gradually withdraw from work in the cyclic load.
2) The improvement in ductility of the polymer matrix of BFRP can obviously reduce matrix crack propagation under static and fatigue loading. With higher ductility and fewer cracks, the long-term fatigue life and residual stiffness of more ductile matrix based BFRP, such as BRV and BSE, are higher than that of BV and BE. The 10 million cycle fatigue strength level

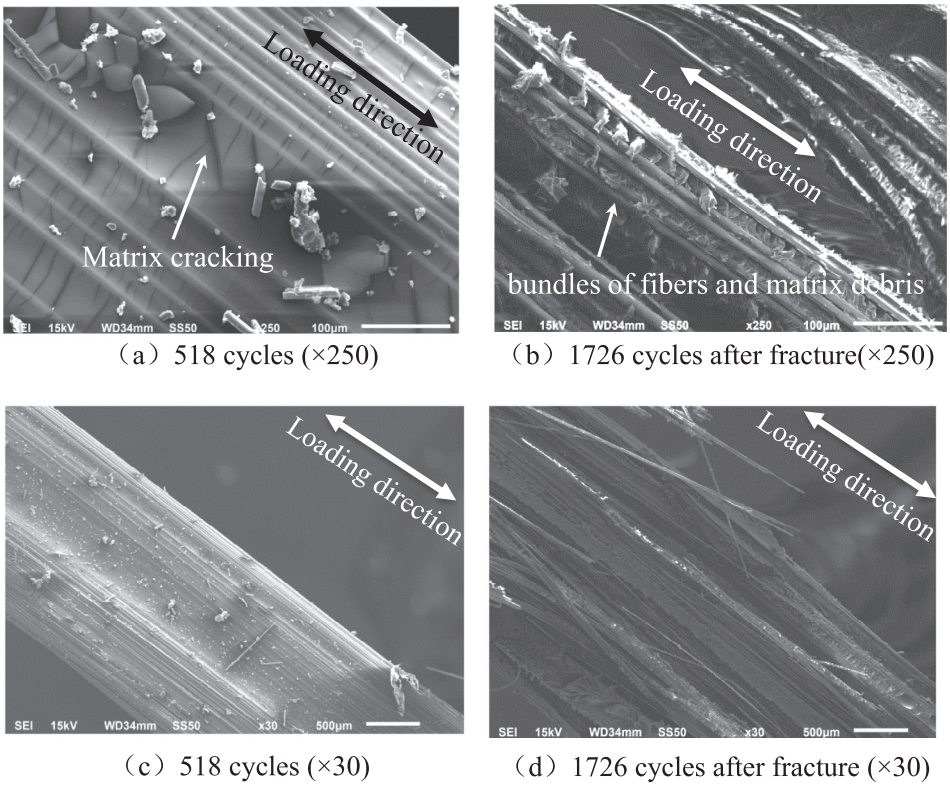

（a）518 cycles (×250)　（b）1726 cycles after fracture(×250)

（c）518 cycles (×30)　（d）1726 cycles after fracture (×30)

Fig. 10. Typical fatigue damage for BRV under maximum fatigue stress of 2087 MPa.

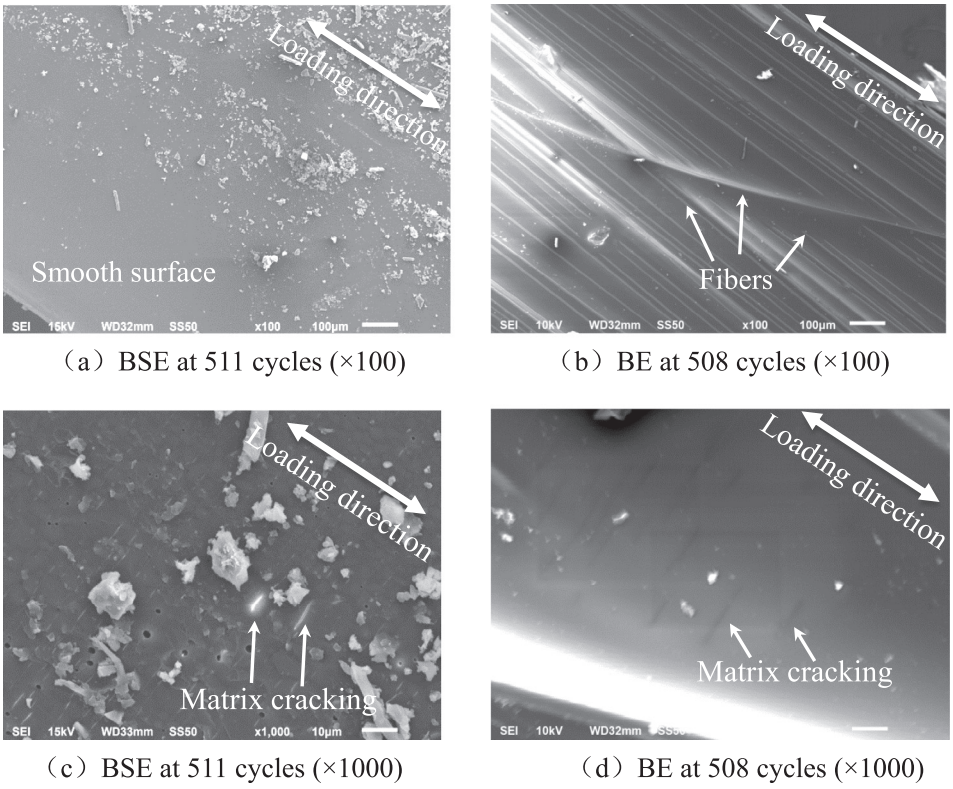

（a）BSE at 511 cycles (×100)　（b）BE at 508 cycles (×100)

（c）BSE at 511 cycles (×1000)　（d）BE at 508 cycles (×1000)

Fig. 11. Typical fatigue damage for BSE and BE under maximum fatigue stress of 2087 MPa.

of vinyl resin based BFRP increased from 69.89% to 75.56% before and after toughening. However, the static strength and short-term fatigue life of BRV and BSE are lower than BV and BE specimens.

3) The slope of the S–N fatigue curve increases with the resin matrix elongation increase for all types of resin tested. The long-term fatigue limit of the BFRP composites can be controlled by matrix cracking and matrix elongation.

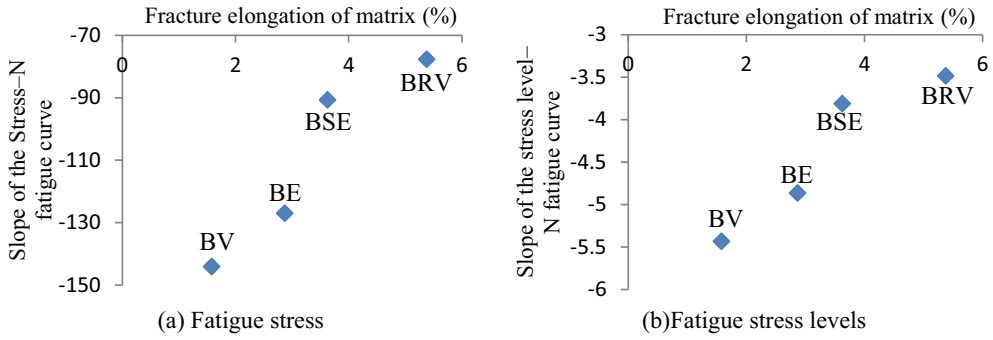

Fig. 12. The relationship of the slope of the S–N curve and polymer matrix elongation.

The results from this study highlighting a clear resin effect in long-term fatigue life of BFRP are based on a limited data set. Additional testing would help quantify these effects and provide more guidance on fatigue life improvement of BFRP products. In the future, more suitable matrix can be studied and used in BFRPs to get BFRP cables, bridge decks or other products longer fatigue life.

CRediT authorship contribution statement

Xing Zhao: Conceptualization, Data curation, Methodology, Investigation, Writing - original draft. **Xin Wang:** Conceptualization, Formal analysis, Funding acquisition, Writing - review & editing, Supervision. **Zhishen Wu:** Conceptualization, Project administration, Writing - review & editing, Supervision. **Jin Wu:** Resources, Writing - review & editing, Supervision.

Declaration of Competing Interest

The authors declare that they have no known competing financial interests or personal relationships that could have appeared to influence the work reported in this paper.

Acknowledgements

The authors gratefully acknowledge the financial support provided by the National Key Research and Development Program of China (2017YFC0703000), the National Natural Science Foundation of China (51678139).

References

[1] Z. Dong, G. Wu, B. Xu, X. Wang, L. Taerwe, Bond durability of BFRP bars embedded in concrete under seawater conditions and the long-term bond strength prediction, Mater. Des. 92 (2016) 552–562.
[2] G. Wu, X. Wang, Z. Wu, Z. Dong, G. Zhang, Durability of basalt fibers and composites in corrosive environments, J. Compos. Mater. 49 (7) (2015) 873–887.
[3] J.W. Shi, H. Zhu, Z.S. Wu, G. Wu, Durability of BFRP and hybrid FRP sheets under freeze-thaw cycling, in: Advanced Materials Research, Trans Tech. Publ., 2011, pp. 3297–3300.
[4] X. Wang, J. Shi, J. Liu, L. Yang, Z. Wu, Creep behavior of basalt fiber reinforced polymer tendons for prestressing application, Mater. Des. 59 (2014) 558–564.
[5] J.W. Shi, W.H. Cao, L. Chen, A.L. Li, Durability of wet lay-up BFRP single-lap joints subjected to freeze–thaw cycling, Constr. Build. Mater. 238 (2020) 117664.
[6] W. Xin, J. Shi, Z. Wu, Z. Zhu, Creep strain control by pretension for basalt fiber-reinforced polymer tendon in civil applications, Mater. Des. (2015).
[7] Z.F. Chen, L.L. Wan, S. Lee, M. Ng, J.M. Tang, M. Liu, L. Lee, Evaluation of CFRP, GFRP and BFRP material systems for the strengthening of RC slabs, J. Reinf. Plast. Compos. 27 (12) (2008) 1233–1243, https://doi.org/10.1177/0731684407084122.
[8] Xin Wang, Zhishen Wu, Evaluation of FRP and hybrid FRP cables for super long-span cable-stayed bridges, Compos. Struct. 92 (10) (2010) 2582–2590, https://doi.org/10.1016/j.compstruct.2010.01.023.
[9] A. Nanni, G. Claure, F.J.D.C.Y. Basalo, O. Gooranorimi, Concrete and composites pedestrian, Bridge 38 (11) (2016) 57–63.
[10] R. Talreja, 5 – Matrix and fiber–matrix interface cracking in composite materials, Modeling Damage Fatigue Failure Compos. Mater. (2016) 87–96.
[11] K.L. Reifsnider, Fatigue of composite materials, Elsevier Science Publishers B. V, Amsterdam, The Netherlands, 1991.
[12] R. Talreja, Fatigue of composite materials: damage mechanisms and fatigue-life diagrams, Proc. R. Soc. A Math. Phys. Eng. Sci. 378 (1775) (1981) 461–475.
[13] X. Zhao, X. Wang, Z. Wu, Z. Zhu, Fatigue behavior and failure mechanism of basalt FRP composites under long-term cyclic loads, Int. J. Fatigue 88 (2016) 58–67.
[14] S. Rassmann, R. Paskaramoorthy, R.G. Reid, Effect of resin system on the mechanical properties and water absorption of kenaf fibre reinforced laminates, Mater. Des. 32 (3) (2011) 1399–1406.
[15] C. Colombo, L. Vergani, M. Burman, Static and fatigue characterisation of new basalt fibre reinforced composites, Compos. Struct. 94 (3) (2012) 1165–1174.
[16] M.R. Ricciardi, I. Papa, A. Langella, T. Langella, V. Lopresto, V. Antonucci, Mechanical properties of glass fibre composites based on nitrile rubber toughened modified epoxy resin, Compos. B Eng. 139 (2018) 259–267.
[17] L.P. Borrego, J.D.M. Costa, J.A.M. Ferreira, H. Silva, Fatigue behaviour of glass fibre reinforced epoxy composites enhanced with nanoparticles, Compos. B Eng. 62 (21) (2014) 65–72.
[18] P.J. Burchill, A. Kootsookos, M. Lau, Benefits of toughening a vinyl ester resin matrix on structural materials, J. Mater. Sci. 36 (17) (2001) 4239–4247.
[19] M. Sheinbaum, L. Sheinbaum, O. Weizman, H. Dodiuk, S. Kenig, Toughening and enhancing mechanical and thermal properties of adhesives and glass-fiber reinforced epoxy composites by brominated epoxy, Compos. B Eng. 165 (2019) 604–612.
[20] J.W. Shi, H. Zhu, J.G. Dai, X. Wang, Z.S. Wu, Effect of rubber toughening modification on the tensile behavior of FRP composites in concrete-based alkaline environment, J. Mater. Civ. Eng. 27 (12) (2015) 04015054.
[21] X. Zhao, X. Wang, Z. Wu, T. Keller, A.P. Vassilopoulos, Effect of stress ratios on tension–tension fatigue behavior and micro-damage evolution of basalt fiber-reinforced epoxy polymer composites, J. Mater. Sci.
[22] ISO 10618:2004(en) Carbon fibre — Determination of tensile properties of resin-impregnated yarn, 2004.
[23] G.C. Sih, X.S. Tang, Z.X. Li, A.Q. Li, K.K. Tang, Fatigue crack growth behavior of cables and steel wires for the cable-stayed portion of Runyang bridge: Disproportionate loosening and/or tightening of cables, 49(1) (2008) 1–25.
[24] V. Barron, M. Buggy, N.H. McKenna, Frequency effects on the fatigue behaviour on carbon fibre reinforced polymer laminates, J. Mater. Sci. 36 (7) (2001) 1755–1761.
[25] ACI Committee 440, Report on fibre reinforced polymer (FRP) reinforcement for concrete structures (ACI 440R-07), 2007.
[26] A.N. Towo, M.P. Ansell, Fatigue of sisal fibre reinforced composites: Constant-life diagrams and hysteresis loop capture, Compos. Sci. Technol. 68 (3–4) (2008) 915–924.
[27] Z. Wu, X. Wang, K. Iwashita, T. Sasaki, Y. Hamaguchi, Tensile fatigue behaviour of FRP and hybrid FRP sheets, Compos. B Eng. 41 (5) (2010) 396–402.
[28] V. Fiore, T. Scalici, G. Di Bella, A. Valenza, A review on basalt fibre and its composites, Compos. B Eng. 74 (2015) 74–94.
[29] ACI committee 440, Guide for the Design and Construction of Externally Bonded FRP Systems for Strengthening Concrete Structures (440.2R-17), 2017.
[30] A.P. Vassilopoulos, T. Keller, Fatigue of Fiber-Reinforced Composites, Springer, London, 2011.
[31] J. Zong, W. Yao, Fatigue life prediction of composite structures based on online stiffness monitoring, J. Reinf. Plast. Compos. 36 (14) (2017) 1038–1057.
[32] K. Senthilnathan, C.P. Hiremath, N.K. Naik, A. Guha, A. Tewari, Microstructural damage dependent stiffness prediction of unidirectional CFRP composite under cyclic loading, Compos. Pt. A-Appl. Sci. Manuf. 100 (2017) 118–127.